Technology and Health Care 7 (1999) 53–61
IOS Press

Evaluating phosphors for use in X-ray image detectors by the effective performance index (EPI) method: application to Eu^{3+} activated yttrium based materials

D. Cavouras [a,*], I. Kandarakis [a], P. Prassopoulos [b], E. Kanellopoulos [a], C.D. Nomicos [c] and G.S. Panayiotakis [d]

[a] *Department of Medical Instrumentation Technology, Technological Educational Institution of Athens, Ag. Spyridonos Street, Aigaleo, 122 10 Athens, Greece*
[b] *Department of Radiology, University Hospital, Medical School, University of Crete, Heraklion, Greece*
[c] *Department of Electronics, Technological Educational Institution of Athens, Ag. Spyridonos Street, Aigaleo, 122 10 Athens, Greece*
[d] *Department of Medical Physics, Medical School, University of Patras, 265 00 Patras, Greece*

Received 28 June 1998
Revised 26 September 1998

Abstract. Phosphor materials used in X-ray image receptors were evaluated by the effective performance index (EPI). EPI describes the dependence of image quality on X-ray to light energy conversion and light diffusion processes. EPI was experimentally determined by means of X-ray luminescence (XLE) and MTF measurements performed on Y_2O_2S:Eu, Y_2O_3:Eu, and YVO_4:Eu phosphors. The spectral compatibility of these materials with optical detectors (films, photocathodes, photodiodes) was also determined. Highest EPI values were obtained for Y_2O_2S:Eu-GaAs combination at mammographic energies. All phosphors could be of use in digital X-ray imaging being adequately compatible to silicon photodiodes employed in digital detectors.

Keywords: Phosphors, X-ray image detectors, X-ray luminescence, MTF

1. Introduction

The performance of X-ray medical image receptors is assessed in terms of their ability to produce high quality images with minimal patient dose burden. Image diagnostic quality and dose burden are both related to the total receptor conversion efficiency (RCE). RCE expresses the ability of the receptor to capture X-ray quanta exiting the patient's body and convert their energy into useful diagnostic signal. This signal may be optical or electronic, depending on the imaging modality, e.g., conventional or digital X-ray imaging and computed tomography [1,12,14]. RCE is the result of a number of signal conversion

*Please address correspondence: Prof. D. Cavouras, Ph.D., 37-39 Esperidon Street, Kallithea 17671, Athens, Greece. Tel.: (+301) 9594 558; Fax: (+301) 5910 975; E-mail: cavouras@medisp.teiath.gr.

processes within the receptor causing a significant reduction in signal energy and image quality. The latter is also affected by diffusion mechanisms that deteriorate signal spatial distribution such as isotropic light emission and optical scattering within the detector phosphor materials [2,14]. While conversion processes determine the total signal energy displayed at the receptor output, diffusion affects its spatial distribution.

In the present study, the effect of phosphor material properties on image receptor performance was studied by defining the phosphor effective performance index (EPI). EPI incorporates the effects of both conversion and diffusion processes on signal energy and image quality respectively and provides a means for comparing the suitability of various phosphors for use in X-ray imaging. Conversion and diffusion processes were expressed by coefficients, with values ranging from 0 to 1, quantitatively describing the degree of image degradation resulting from each process. EPI was evaluated for three europium activated phosphors (Y_2O_2S:Eu, Y_2O_3:Eu, and YVO_4:Eu) [2,11] employed in the form of fluorescent layers (screens).

2. Materials and methods

2.1. Conversion mechanisms

The total conversion efficiency C_{tot} of an X-ray image receptor may be defined as the product of specific conversion efficiencies C_i:

$$C_{\text{tot}} = \prod_{i=1}^{n} C_i, \quad i = 1, 2, \ldots, 6. \tag{1}$$

In a phosphor – optical detector receptor, the following efficiencies may be distinguished:

C_1 is the phosphor efficiency for conversion of the incident X-ray quanta energy into absorbed energy, often called quantum detection efficiency (QDE) [9,13].

C_2 is the phosphor intrinsic efficiency for conversion of the absorbed X-ray energy into energy of light photons created within the phosphor [9,13].

C_3 is the efficiency for conversion of the energy of light photons created in stage C_2 into emitted light energy (light transmission efficiency) [9,13].

C_4 is the efficiency for conversion of the emitted light photons energy into energy matched by the spectral sensitivity of the optical detector [4].

C_5 is the geometric conversion efficiency giving the fraction of energy of detectable light photons that arrive at the optical detector input [6,12,14].

C_6 is the quantum conversion efficiency of the optical detector giving the number of output signal carriers (film developed grains or electrons in photodiode output) per unit of optical energy incident on the optical detector [6,12].

Therefore, for real image receptors, the specific conversion efficiencies C_i are always lower than unity resulting in $C_{\text{tot}} < 1$. For the special case of an ideal image receptor $C_i = C_{\text{tot}} = 1$.

The product of the first three conversion efficiencies C_1, C_2, C_3 has been defined [10,13] as the X-ray luminescence efficiency (XLE) of phosphors. XLE may be considered as the efficiency of the phosphor to convert the incident X-ray energy into emitted light. Thus:

$$\text{XLE}(E) = \prod_{1}^{3} C_i = \frac{\Psi_\lambda(E_\lambda)}{\Psi_{\text{X}}(E)}, \tag{2}$$

where Ψ_λ is the emitted light flux, E_λ is the energy of the emitted light photons, Ψ_X is the incident X-ray energy flux, E is the energy of the X-ray quanta.

Since polyenergetic beams are used in X-ray imaging, XLE must be written by expressing X-ray energy and light energy fluxes in integral form

$$\mathrm{XLE}(E_0) = \frac{\Psi_\lambda(E_0, E_\lambda)}{\Psi_X(E_0)} = \frac{\int_0^{E_0} [\mathrm{d}\Psi_X(E)/\mathrm{d}E]\mathrm{XLE}(E)\,\mathrm{d}E}{\int_0^{E_0} [\mathrm{d}\Psi_X(E)/\mathrm{d}E]\,\mathrm{d}E}, \tag{3}$$

where, E_0 is the maximum energy of the X-ray spectrum determined by the tube voltage. $[\mathrm{d}\Psi_X(E)/\mathrm{d}E]$ is the spectral density in $\mathrm{W\,m^{-2}\,keV^{-1}}$. XLE was experimentally determined by measuring the emitted light flux using an EMI 9558QB photomultiplier connected to a Cury 401 electrometer and the incident X-ray exposure rate by a type No 23333 PTW dosemeter. Exposure data were converted into X-ray flux values using the conversion formula [5,7]:

$$\Psi_X = \dot{X}\frac{\lfloor W_{air}/e \rfloor}{[\mu_{en}/\rho]_{air}}, \tag{4}$$

where W_{air} is the mean energy required to produce an ion pair in air, e is the electron charge, and $[\mu_{en}/\rho]_{air}$ is the mass energy absorption coefficient of air.

C_4 was determined using the formula [2,4]:

$$C_4 = \frac{\int_{\lambda_1}^{\lambda_2} \overline{\Psi}_\lambda(\lambda) S_{OD}(\lambda)\,\mathrm{d}\lambda}{\int_{\lambda_1}^{\lambda_2} S_{OD}(\lambda)\,\mathrm{d}\lambda}, \tag{5}$$

where, $\overline{\Psi}_\lambda$ is the normalized emission spectrum of the phosphor material measured with an Oriel 7240 monochromator and $S_{OD}(\lambda)$ is the spectral sensitivity distribution of the optical detector. For the optical detectors considered in this study $S_{OD}(\lambda)$ were obtained from manufacturer's data.

C_5 and C_6 were considered independent of the phosphor material used. Thus, for the purposes of this study, where only phosphor behavior is examined, C_5 and C_6 were set equal to unity.

2.2. Diffusion mechanisms

Diffusion mechanisms take place during the previously described conversion stages. In the first stage of X-ray detection, diffusion is expressed by the effects of X-ray scattering and K-characteristic X-ray generation. In the second stage of X-ray energy into light energy conversion, diffusion is expressed by the isotropic emission of light within the phosphor mass, which widens the spatial distribution of photons at the screen output. In the third stage of light transmission through the phosphor mass, diffusion is mainly expressed by optical scattering within the phosphor and optical reflection effects at the screen – optical coupling interfaces.

Image degradation due to diffusion processes may be described by the modulation transfer function (MTF) [1,8]. The latter expresses the signal modulation and contrast as a function of spatial frequency ω. Instead of a function, diffusion image degradation may also be conveniently described by a single index in terms of the noise equivalent passband [3] N_e as:

$$N_e = \int_0^{\omega_{max}} \left[T_{tot}(\omega)\right]^2 \mathrm{d}\omega, \tag{6}$$

where $\omega_{\max}$ represents the maximum measured spatial frequency and $T_{\text{tot}}(\omega)$ is the overall MTF of the image receptor:

$$T_{\text{tot}} = \prod_{i=1}^{n} T_i(\omega), \quad i = 1, 2, \ldots, 6, \tag{7}$$

where $T_i(\omega)$ represents the MTF corresponding to the conversion stage i. For ideal image receptors $T_i(\omega) = 1 = T_{\text{tot}}(\omega)$.

Furthermore, N_{e} may be normalized to take values from 0 to 1 by defining the image sharpness index S as:

$$S = \frac{\int_0^{\omega_{\max}} [T_{\text{tot}}(\omega)]^2 \, \mathrm{d}\omega}{\int_0^{\omega_{\max}} [T_{\text{tot}}(\omega)]_{\text{id}}^2 \, \mathrm{d}\omega} = \frac{\int_0^{\omega_{\max}} \left[\prod_{i=1}^{0} T_i(\omega)\right]^2 \mathrm{d}\omega}{\omega_{\max}}, \tag{8}$$

where subscript id denotes the MTF of an ideal image receptor (e.g., MTF $= 1$).

The sharpness index S was evaluated using Eq. (8) and MTF data. MTF was measured employing the square wave response function (SWRF) method [1,2,8,10]. A typ-53 MTF test pattern (Nuclear Associates) with spatial frequencies from 0.25 to 10 lp/mm was imaged using the screens in contact with an Agfa Scopix LT2B film. The film images were digitized on a Microtec Scanmaker II SP (1200×1200 dpi) scanner. SWRFs were obtained by averaging 64 successive traces vertically directed to the pattern bars. Screen film characteristic curves were also obtained to correct for film non-linearities [1]. Final results were obtained employing Coltman's formula [1,8]:

$$\text{MTF}(\omega, t) = \frac{\pi}{4} \sum_{k=1}^{\infty} b_k \frac{\text{SWRF}\big[(2k-1)\omega, t\big]}{(2k-1)}, \tag{9}$$

where t is the screen coating weight,

$$b_k = 0, \quad \text{for } m < n$$
$$b_k = (-1)^n (-1)^{k-1}, \quad \text{for } m = n.$$

n is the number of prime factors other than unity in $(2k-1)$, m is the number of prime factors other than unity which appear only once in $(2k-1)$ [8].

In a manner analogous to XLE determination, only the phosphor MTF was considered and consequently $T_5(\omega)$ and $T_6(\omega)$ in Eq. (7) were set equal to unity. Thus, MTF in (10) corresponds to the product of the MTFs (see Eq. (7)) of the first three stages, i.e.,

$$T_{\text{tot}} = \prod_{i=1}^{3} T_i(\omega).$$

Finally, the effective performance index may be defined as:

$$\text{EPI} = C_{\text{tot}} S. \tag{10}$$

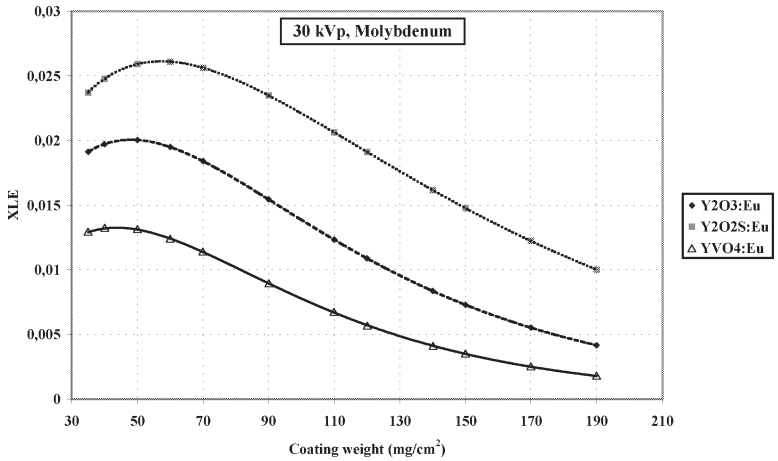

Fig. 1. Variation of the X-ray luminescence efficiency (XLE) of Y_2O_2S:Eu, Y_2O_3:Eu and YVO_4:Eu phosphors with screen coating weight, measured at 30 kVp using molybdenum target X-rays.

2.3. Phosphor materials used

XLE, C_4, MTF and consequently C_{tot} and S were determined for Y_2O_2S:Eu, Y_2O_3:Eu and YVO_4:Eu phosphors, which emit red light due to the presence of the Eu^{3+} activator. These phosphors have been supplied in powder form with approximate grain diameter 7 μm, and were used as fluorescent layers (phosphor screens). The screens were prepared by a sedimentation technique [2,9–11] and they were of granular form with a packing density slightly exceeding 50% similar to those commercially available. The coating weights (thickness in mg/cm^2) of the screens produced were 35–210 mg/cm^2. Phosphor EPI were determined for X-ray tube voltages of 30, 80 and 120 kVp, which are very often employed in both conventional and digital X-ray imaging.

3. Results

Figure 1 shows the variation of the X-ray luminescence efficiency of Y_2O_2S:Eu, Y_2O_3:Eu and YVO_4:Eu phosphors with screen coating weight, measured at 30 kVp. Measurements were performed on a molybdenum target X-ray tube employed in mammographic imaging. Y_2O_2S:Eu phosphor was found clearly better than the other materials for the whole range of screen coating weights. Peak XLE value was obtained for the 60 mg/cm^2 screen but the XLE values of the 40, 50 and 70 mg/cm^2 screens were found very close to maximum. In the case of Y_2O_3:Eu and YVO_4:Eu phosphors, maximum XLE values were obtained at 50 and 40 mg/cm^2 respectively and screens in the range 35–60 mg/cm^2 displayed XLEs close to the local maxima.

Figure 2 shows the variation of XLE with screen coating weight measured at 80 kVp using a tungsten target tube. Highest XLE values were obtained for Y_2O_2S:Eu, at 140 mg/cm^2, for Y_2O_3:Eu at 110 mg/cm^2 and for YVO_4:Eu at 90 mg/cm^2. However, screens with coating weight up to $\pm$30 mg/cm^2 from the local XLE maxima were found very close to the corresponding XLE highest values.

The same XLE behavior was observed at 120 kVp as shown in Fig. 3. Phosphor peak XLE values were obtained for thicker screens (110, 120, 170 mg/cm^2) while all XLE values were lower than those measured at 30 and 80 kVp.

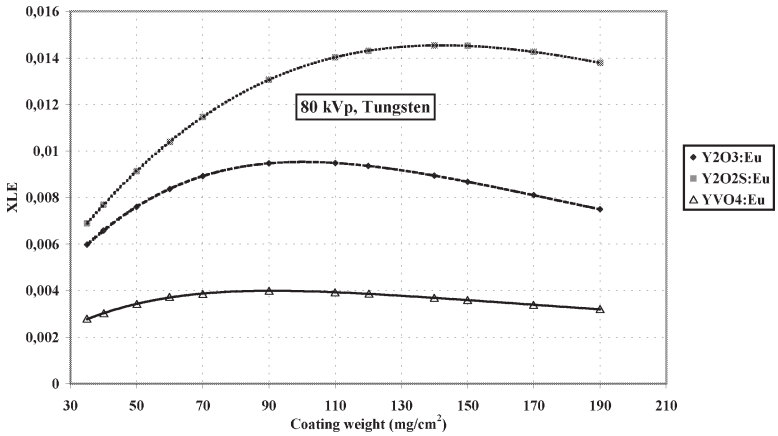

Fig. 2. Variation of the X-ray luminescence efficiency (XLE) of Y_2O_2S:Eu, Y_2O_3:Eu and YVO_4:Eu phosphors with screen coating weight, measured at 80 kVp using tungsten target X-rays.

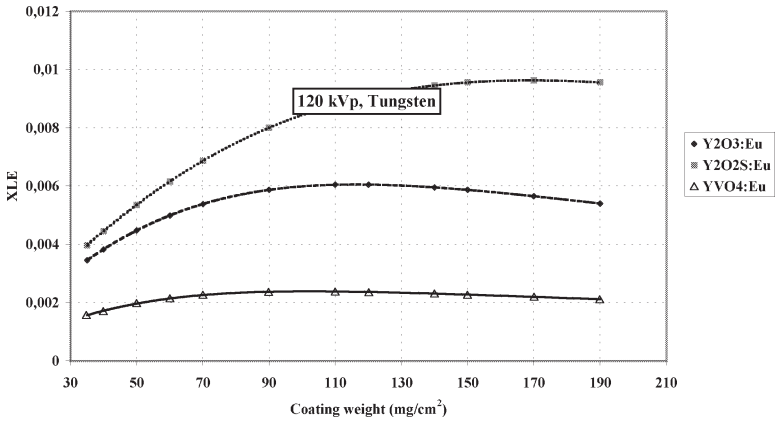

Fig. 3. Variation of the X-ray luminescence efficiency (XLE) of Y_2O_2S:Eu, Y_2O_3:Eu and YVO_4:Eu phosphors with screen coating weight, measured at 120 kVp using tungsten target X-rays.

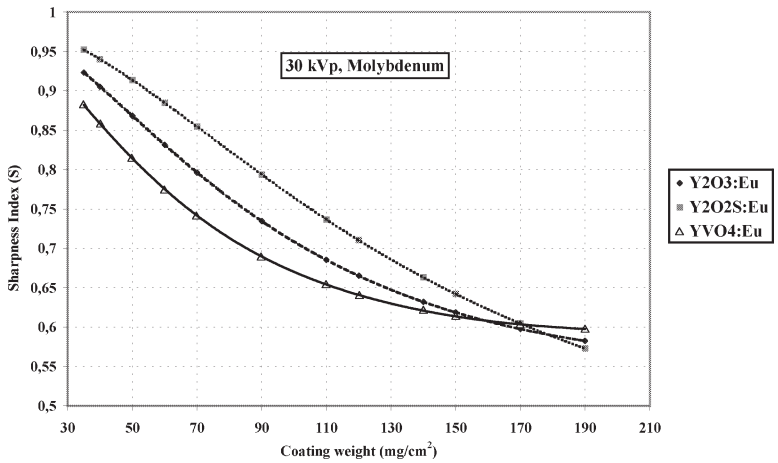

Fig. 4. Variation of the sharpness index (S) with coating weight, determined at 30 kVp using molybdenum target X-rays.

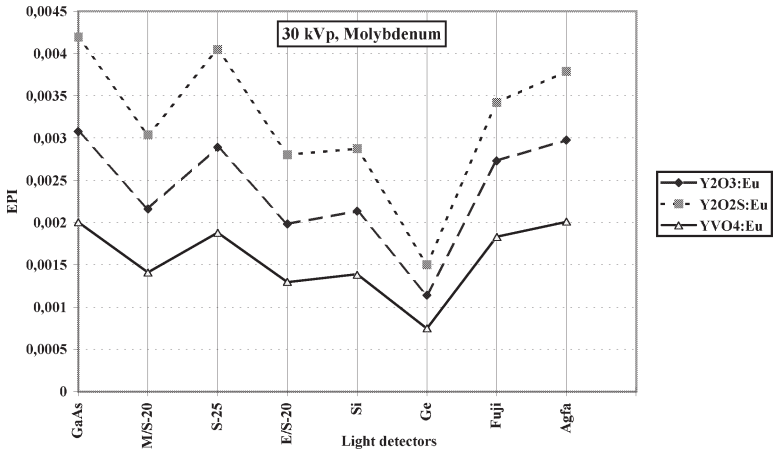

Fig. 5. Effective performance index (EPI) of Y_2O_2S:Eu, Y_2O_3:Eu and YVO_4:Eu phosphors in combinations with various optical detectors, determined at 30 kVp using molybdenum target X-rays.

Figure 4 shows the variation of the sharpness index (S) with coating weight determined at 30 kVp. S was found higher for Y_2O_2S:Eu for coating weights up to 170 mg/cm^2 while for thicker coatings YVO_4:Eu was better.

Figure 5 presents the effective performance index at 30 kVp of the three phosphors corresponding to combinations with various optical detectors. The optical detectors considered were the following:

1. The extended sensitivity E/S-20, the modified sensitivity M/S-20, the S-25 and the GaAs photocathodes used in image intensifiers for conventional fluoroscopy, digital angiography, digital mammography, etc.
2. The Agfa Scopix LT2B and the LI-HM Fuji films normally employed with laser cameras connected to digital imaging systems. However, since these films are very sensitive to red light they were used in this study in combination with the Eu activated phosphors to simulate conventional radiographic film-screen cassettes.
3. The silicon (Si) and germanium (Ge) photodiodes: Si photodiodes coupled to phosphors are used in digital radiography and computed tomography detectors.

Highest EPI values were obtained for the Y_2O_2S:Eu/GaAs and the Y_2O_2S:Eu/S-25 combinations. EPI was also found very high for the Y_2O_2S:Eu combined with the Agfa Scopix film. The latter and the GaAs photocathode also gave best results in combinations with the Y_2O_3:Eu and YVO_4:Eu phosphors, which were also very well combined with the S-25 photocathode. Additionally, YVO_4:Eu was very good when combined with the LI-HM Fuji film. The same phosphor–optical detector combinations gave highest EPI values at 80 and 120 kVp (see Figs. 6 and 7). However, these values were lower than those shown in Fig. 5 obtained at 30 kVp.

4. Discussion

XLE data shown in Fig. 1 are interesting for mammographic applications since screens between 35 and 60 mg/cm^2, exhibiting high XLE, may also produce high resolution images, which is very important in breast imaging [2,6]. For thicker screens XLE decreases continuously due to light attenuation effects causing a respective decrease in the values of light transmission efficiency (C_3 in Formulas (1) and (2)).

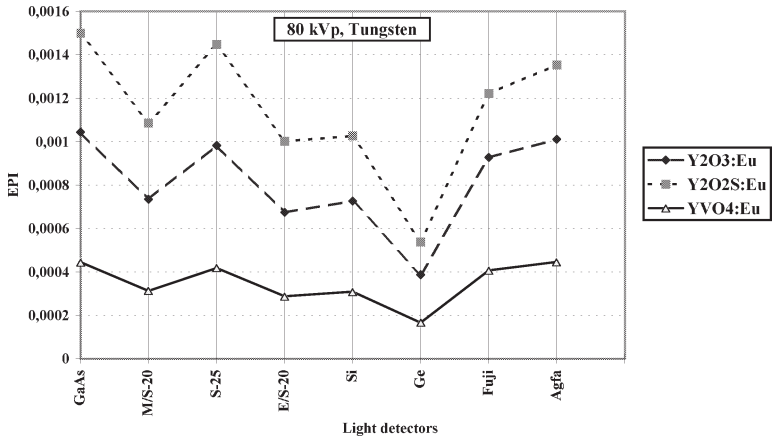

Fig. 6. Effective performance index (EPI) of Y_2O_2S:Eu, Y_2O_3:Eu and YVO_4:Eu phosphors in combinations with various optical detectors, determined at 80 kVp using tungsten target X-rays.

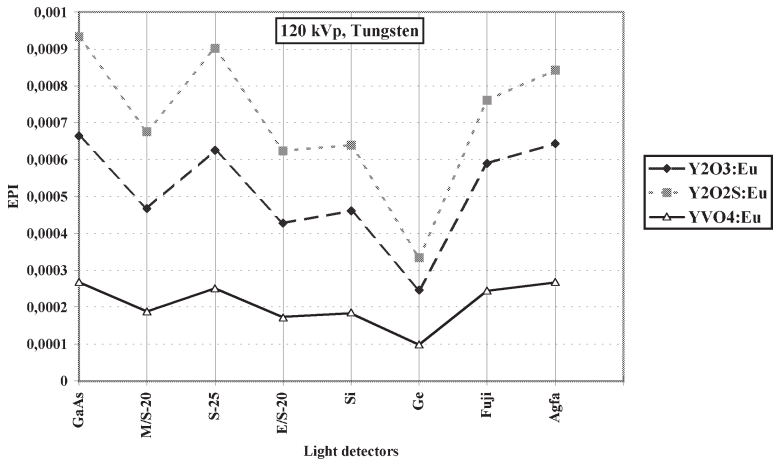

Fig. 7. Effective performance index (EPI) of Y_2O_2S:Eu, Y_2O_3:Eu and YVO_4:Eu phosphors in combinations with various optical detectors, determined at 120 kVp using tungsten target X-rays.

At 80 kVp (Fig. 2) XLE was found higher at relatively thick screens, since 80 kVp X-rays are able to penetrate thick phosphor layers before their absorption. Thus, thick phosphor screens can capture more 80 kVp X-ray quanta than thin screens and can produce more light photons, which then travel rather short distances to escape the screens from the opposite side suffering less attenuation. However, peak XLE values were lower than those obtained with 30 kVp X-rays. This is because the latter are practically totally absorbed even at thin phosphor layers resulting in higher light output at low coating weights.

As it was expected, image degradation due to diffusion processes increases with phosphor thickness (see Fig. 4). This is because laterally emitted or scattered light photons travel longer distances within the phosphor mass. This broadens the spatial distribution of light at the screen emitting surface which reduces image sharpness.

The results for EPI shown in Figs. 5–7 show that Y_2O_2S:Eu, Y_2O_3:Eu and YVO_4:Eu could be employed in both conventional and digital fluoroscopy and in radiography using conventional screen-film combinations or digital detectors based on image intensifier technology. For all phosphors the combina-

tions with the Si photodiode were better than with the Ge photodiode. The EPI values corresponding to Si detector are satisfactory suggesting that the phosphors studied could be considered for use in digital radiography using CCD arrays coated with phosphor screens.

EPI is a simple method to evaluate and compare the imaging performance of various phosphor–optical detector combinations at various X-ray exposure conditions. The advantage of the method is that it combines in a single dimensionless index both primary image brightness (or light intensity) and spatial resolution (or image sharpness).

A limitation of the EPI method is that it does not include any information on image noise or signal to noise ratio (SNR) associated with the output image. However, this type of information may be indirectly estimated from EPI values since SNR depends strongly on quantum detection efficiency (C_1 in Formula (1)) and on XLE [10].

Acknowledgment

This study is dedicated to the memory of Prof. G.E. Giakoumakis, leading member of our team, whose work on phosphor materials has inspired us to continue.

References

[1] G.T. Barnes, The use of bar pattern test objects in assessing the resolution of film/screen systems', in: *The Physics of Medical Imaging: Recording System, Measurements and Techniques*, A.G. Haus, ed., American Association of Physicists in Medicine, New York, 1979, pp. 138–151.
[2] D. Cavouras, I. Kandarakis, G.S. Panayiotakis, E.K. Evangelou and C.D. Nomicos, An evaluation of the Y_2O_3:Eu^{3+} scintillator for application in medical X-ray detectors and image receptors, *Med. Phys.* **23** (1996), 1965–1975.
[3] A.L. Evans, *The Evaluation of Medical Images*, A. Hilger Ltd., Bristol, UK, 1981, pp. 45–46.
[4] G.E. Giakoumakis, Matching factors for various light-source-photodetector combinations, *Appl. Phys.* **A52** (1991), 7–9.
[5] J.R. Greening, Fundamentals of radiation dosimetry, in: *Medical Physics Handbooks*, Institute of Physics, London, 1985, p. 15.
[6] A.M. Gurwich, Luminescent screens for mammography, *Radiat. Meas.* **24** (1995), 325–330.
[7] W.R. Hendee, *Medical Radiation Physics*, Year Book Medical Publishers, Chicago, 1970, pp. 145–148.
[8] ICRU, Modulation transfer function of screen-film systems, ICRU Report 41, 1986.
[9] I. Kandarakis, D. Cavouras, G.S. Panayiotakis and C.D. Nomicos, Evaluating X-ray detectors for radiographic applications: a comparison of ZnSCdS:Ag with Gd_2O_2S:Tb and Y_2O_2S:Tb screens, *Phys. Med. Biol.* **42** (1997), 1351–1373.
[10] I. Kandarakis, D. Cavouras, G.S. Panayiotakis, D. Triantis and C.D. Nomicos, An experimental method for the determination of spatial frequency dependent detective quantum efficiency (DQE) of scintillators used in X-ray imaging detectors, *Nucl. Instr. Meth. Phys. Res.* **399** (1997), 335–342.
[11] I. Kandarakis, D. Cavouras, G.S. Panayiotakis, D. Triantis and C.D. Nomicos, Europium-activated phosphors for use in X-ray detectors of medical imaging systems, *Eur. Radiol.* **8** (1998), 313–318.
[12] A. Karellas, L.J. Harris, H. Liu, M.A. Davis and C.J. D'Orsi, Charge-coupled device detector: performance considerations and potential for small-field mammographic imaging applications, *Med. Phys.* **19** (1992), 1015–1023.
[13] G.W. Ludwig, X-ray efficiency of powder phosphors, *J. Electrochem. Soc.* **118** (1971), 1152–1159.
[14] M.J. Yaffe and J.A. Rowlands, X-ray detectors for digital radiography, *Phys. Med. Biol.* **42** (1997), 1–39.